FINE MESH ANALYSIS BY USE OF ISENTROPIC SURFACES

E. Reimer
Free University Berlin

1. INTRODUCTION

Meteorological observations are irregularly distributed in space and time and have different qualities. The purpose of numerical analysis schemes is to produce a representation of these variables on a regular grid. They may be used for initialisation of numerical forecast models or for diagnostic purposes.

Here we use the statistical interpolation scheme, as proposed by Gandin (1963) or Eddy (1967), where the autocorrelation curves of the horizontally distributed variables are used to determine gridpoint estimates by linear regression. These interpolation schemes have been designed for scalar fields.

Today there are more sophisticated schemes which interpolate simultaneously different variables (e.g. Schlatter (1975). Such multivariate schemes are especially used for analysing the fields of geopotential and wind components, where the geostrophic correlation is usually used instead of observed cross-correlation functions.

By using broad-scale numerical weather prediction models along with asynoptic observations, statistical interpolation has been expanded from three to four dimensions by merging data into the on-going numerical forecast (Lorenc (1980)). Such schemes are also very effective in sparse data regions.

When analysing fine scale features some problems arise because the observations are too widespread and the correlation functions are not generally defined at small lags. Moreover, the geostrophic relationship is only appropriate in relation to broad scales.

Therefore a scheme has been tested which overcomes these problems by dividing the analysis procedure into a broad-scale part and a fine-mesh correction. As a vertical coordinate, potential temperature (virtual potential temperature) has been chosen, as used by Bleck (1975) or Shapiro (1975), because it promises a more favourable vertical resolution than other coordinates. The vertical resolution varies with local stability of temperature, so that special features (like fronts) are represented in a more adequate manner.

2. DESCRIPTION OF MODEL

The variables analysed are:

Montgomery potential	$M = C_p T + \Phi$
Exner function	$\pi = (p/1000)^{2/7}$
stability	$\Delta\pi$
wind vector components and relative humidity,	

which are determined on 24 isentropic levels, beginning at 240 K below the ground up to 560 K in the stratosphere.

Also the ground surface is included and, instead of static stability, the potential temperature at the ground is determined. The analysed pressure at the ground is unreduced, so that its analysis represents the orography as described by the observational network. All other ground variables are transferred to the isentropic coordinate system by using the surface potential temperature and pressure.

The broad-scale features are given by the operational 4-dimensional analysis from German Weather Service, DWD, (Kästner (1974)),where massfield, temperature and relative humidity are analysed on 7 pressure-levels and at the sea-surface for a rectangular grid with 254 km resolution at 0°N. These analyses are transformed to isentropic surfaces for the area of interest. The broad-scale description of static stability and the components of wind are derived using a scheme described by Cressman (1959).

The area of interest is shown in Fig.6 and has a horizontal resolution of 64 km at 60N with 81 x 81 gridpoints.

After telescoping, gradually smoothing and simple vertical adjustment the differences between observations and the first guess are used for further statistic interpolation.

The data used are radiosonde, surface and pilot observations. The operational satellite data (SATEM) are not used because they represent larger scales, already included in the operational DWD analyses.

3. BASIC EQUATIONS

The statistical scheme used here is univariate $f_o + d_o = f_{oo} + \Delta f_o$ where f_o is the exact value, d_o the error, f_{oo} the first guess and Δf_o the deviation at gridpoints. For observations $f_i + d_i = f_{oi} + \Delta f_i$; f_{oo} and f_{oi} are large scale analysed and 'observed' values (which are assumed to be exact) while Δf_o and Δf_i represent smaller scale variations and errors.

The linear relationship used is

$$\Delta f_o = \sum_1^8 \alpha_i \, \Delta f_i \tag{1}$$

It is assumed that

$$E = \overline{(\Delta f_{o,result} - \Delta f_{oi})^2} = \min. \tag{2}$$

The weights α_i are given by

$$\sum_1^8 \alpha_i \, m_{ij} + \alpha_i \, e_i = m_{oj} \quad (j = 1,8) \tag{3}$$

where $$m(r_i - r_j) = \frac{\Delta f_i \; \Delta f_j}{\sqrt{\Delta f_i^2 \; \Delta f_j^2}}$$

is the autocorrelation curve and e_i mainly represents observational error variance, normalized by the observed variance.

At the moment, the correlation curve is determined synoptically for each numerical analysis, so that assumptions of isotropy and homogeneity are acceptable. More sophisticated schemes for Montgomery potential and wind components are no longer used because the shape of the small-scale functions is too uncertain.

Fig. 1 shows an autocorrelation curve for the Montgomery potential, where the dots represent values for 0.4-d classes (d - grid resolution) and the analytical function is given by Hermite functions (Reimer, 1980). The first zero is located near lag-5d, because this function describes small scales features. The value at lag-0 is relatively low; this implies that only about 50% of the variance is usable for the determination of the corrections at gridpoints. But one has to realize that all errors are included.

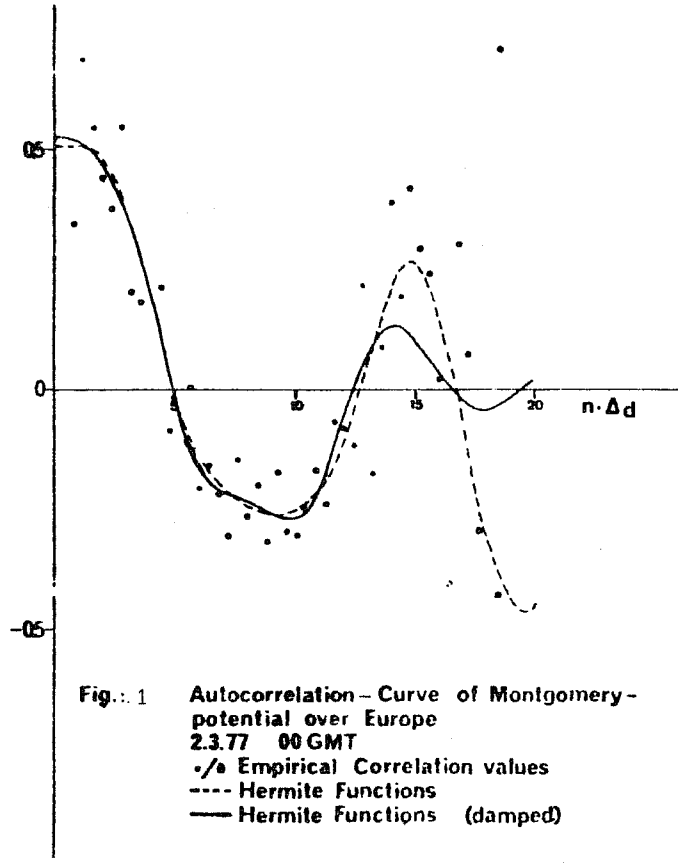

Fig.: 1 Autocorrelation-Curve of Montgomery-potential over Europe
2.3.77 00 GMT
•/• Empirical Correlation values
---- Hermite Functions
—— Hermite Functions (damped)

When autocorrelation functions for radiosonde and pilot-observations are determined for a fine mesh (64 km resolution), problems arise because the low distance classes are not generally defined. Therefore autocorrelation values of the corresponding surface observations are used to complete the tropospheric functions, which are assumed to be independent of height.

Vertical adjustment of stability, Exner function and Montgomery potential is achieved by a simple variational approach. The values at the ground are inserted as additional points with fixed potential temperature.

The relative humidity and the wind components of all gridpoints below the ground are set equal to the value at the ground. The adjustment between ground and isentropic variables in the lower troposphere is also done using a variational approach which ensures that vertical derivatives calculated on isentropic surfaces are realistic.

In the following examples only one correction scan has been employed. However, a second scan generally leads to a smoother and more consistent representation of the variables. Such a second scan should not be considered as artificial since

EXAMPLE

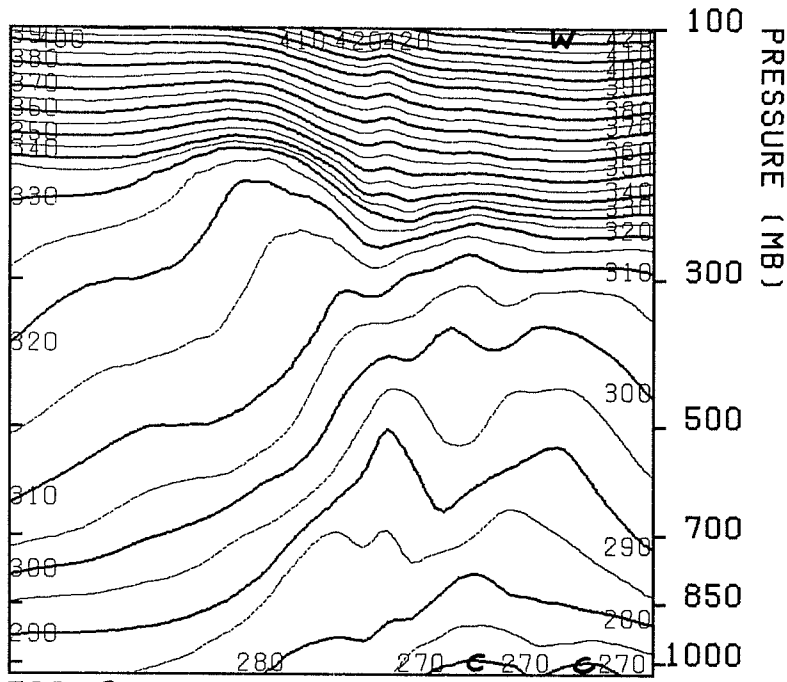

FIG. 2 . POT.TEMPERAT. DGR C.
ANALYSIS 12 GMT 19. 1.1981

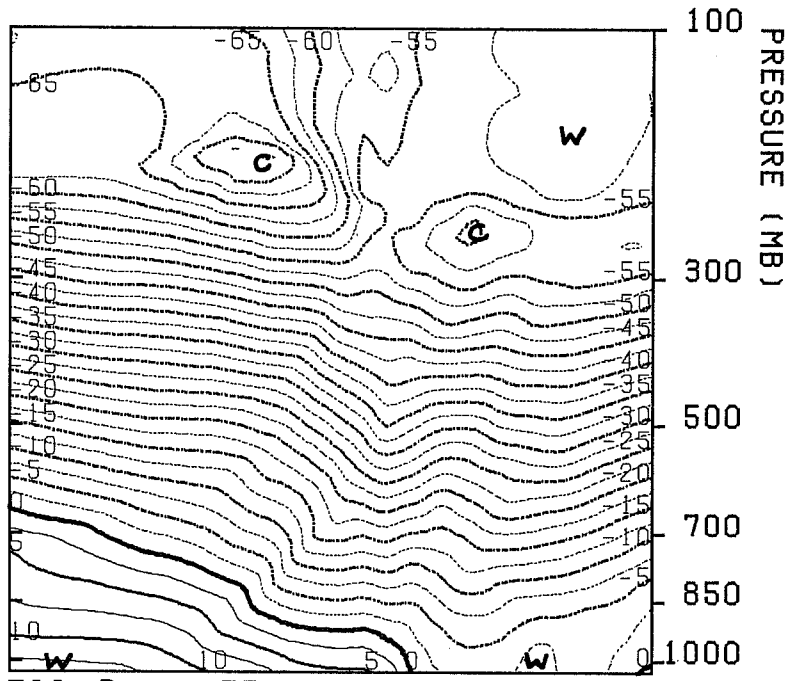

FIG. 3 . TEMPERATURE DGR C.
ANALYSIS 12 GMT 19. 1.1981

West-east cross sections of potential temperature and temperature.

Location is given in Fig. 6.

there are many uncertainties in the statistical scheme and in the observations.

Finally, the variables are transformed from isentropic to pressure coordinate by linear interpolation with the Exner function. On isentropic surfaces all variables are defined below the ground from the beginning. These gridpoints are included in the scheme, so that no special problems arise at the ground during vertical interpolation.

Further adjustment of wind and massfield is done in a way mentioned by Tarbell et al. (1981), where the divergent part of the wind field is derived using the omega equation. Because that step is not a direct part of analysis, it is not described here.

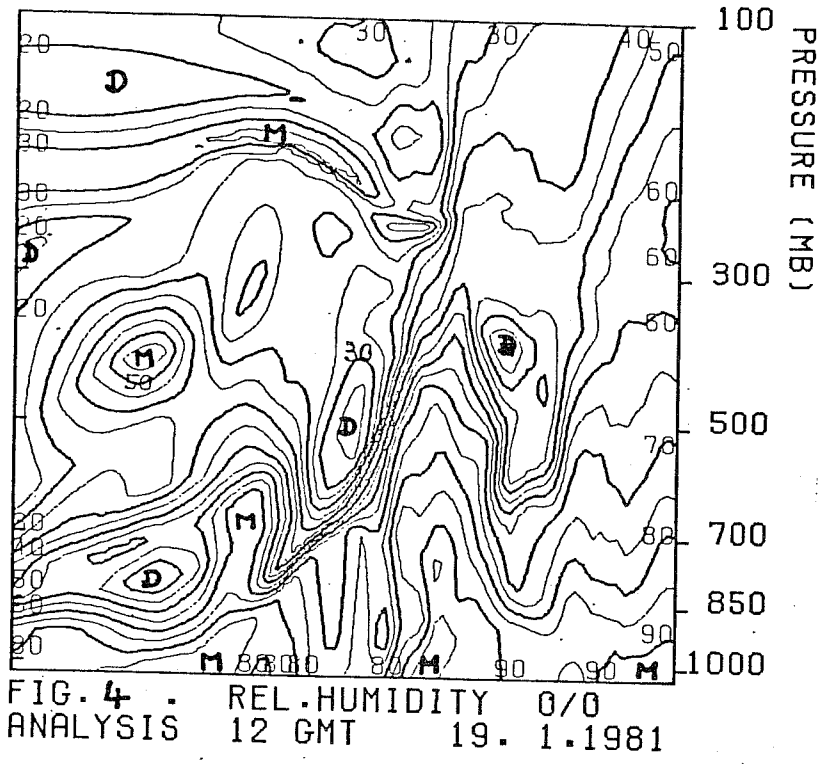

West-East cross section of relative humidity. Location is given in Fig. 6.

4. AN EXAMPLE

To give an example of the special advantages incurred by using isentropic coordinate, Figs. 2 to 4 display vertical cross sections over Central Europe through a frontal zone. Comparing temperature and potential temperature we find that isentropic surfaces envelope the frontal zone for more than 1000 km, while relative humidity shows strong gradients associated with the sharp isothermal layer. Such features are consistently observed when interpolation is done on sloping isentropic surfaces. The same statement is true for the analyses of wind components.

Fig. 5 lag-0 values and variances for different analysis steps

	DWD	Iter.0	Iter.1 Error 10%	Iter.1 Error none	
Montg.Pot.	-.03	.01	.03	-.11	lag-0
	.23	.23	.21	.22	variance
Exner Funct.	.66	.69	.31	.07	lag-0
	.11	.10	.05	.04	variance
Stability	.79	.74	.13	.09	lag-0
	.72	.90	.34	.29	variance

Fig. 5 shows the mean variances and lag-0 values of autocorrelation curves for Montgomery potential, Exner function and stability for all tropospheric isentropic surfaces for broadscale analyses (DWD), adjusted broadscale analyses (Iter.0) and final analyses (Iter.1) with different assumptions about observational errors.

In most of the test cases no autocorrelation is derivable for the Montgomery potential, because the dominant part of the full observed variance is explainable by broadscale features.

However, the Exner function and static stability show relatively high autocorrelations at lag-0 and the variances and correlation values of fine mesh analyses (iter.1) show the improvement in the analyses caused by one correction step.

Assuming that all observations are exact (e = 0 in eq.(3)), the observations are fitted very well, but severe problems arise due to unrealistic error fields in the space between.

Figs. 6 to 9 display geopotential height and temperature on the 1000 mb level for the DWD analysis (6 and 7) and for the fine mesh scheme (8 to 9). Both variables show improvement, especially in mountainous regions such as Scandinavia and the Alps. As an example of the analysis of the wind vector, Fig. 10 shows the rotational part for the interpolated 1000 mb level. The streaming around the Alps (combined with the small mountain effects in the mass and temperature fields) and the sharp horizontal gradients at the Scandinavian coast are a direct result of combining isentropic and surface data.

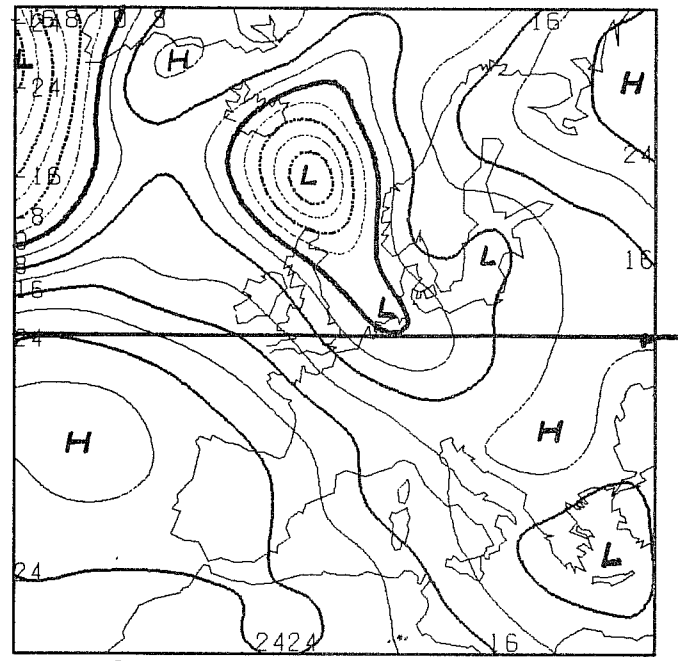

FIG. 6 . GEOP.-HEIGHT GDM
ANALYSIS 12 GMT 19. 1.1981
PRESSURE-LEVEL 1000. MB

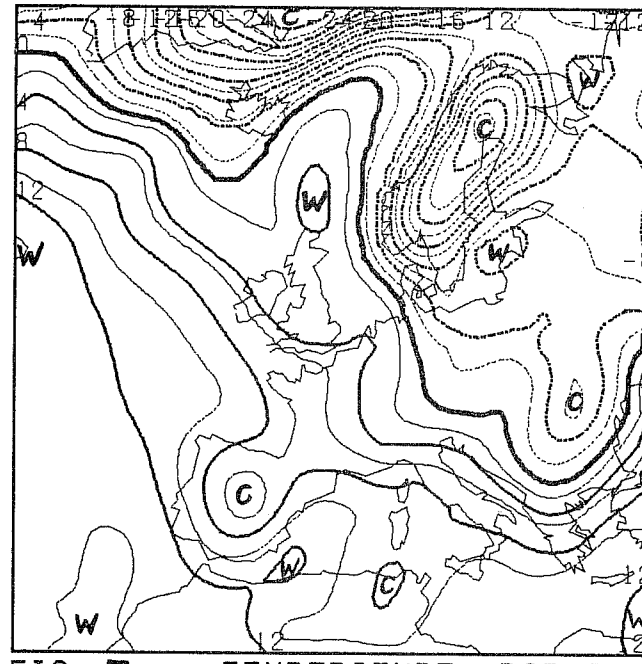

FIG. 7 . TEMPERATURE DGR C.
ANALYSIS 12 GMT 19. 1.1981
PRESSURE-LEVEL 1000. MB

Geopotential height and temperature at 1000 mb as analysed by DWD operational analysis scheme.

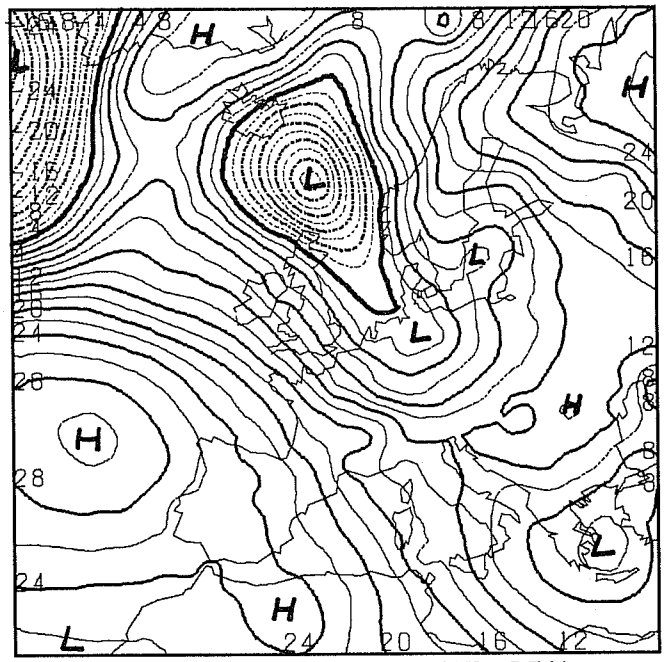

FIG. 8 . GEOP.-HEIGHT GDM
ANALYSIS 12 GMT 19. 1.1981
PRESSURE-LEVEL 1000. MB

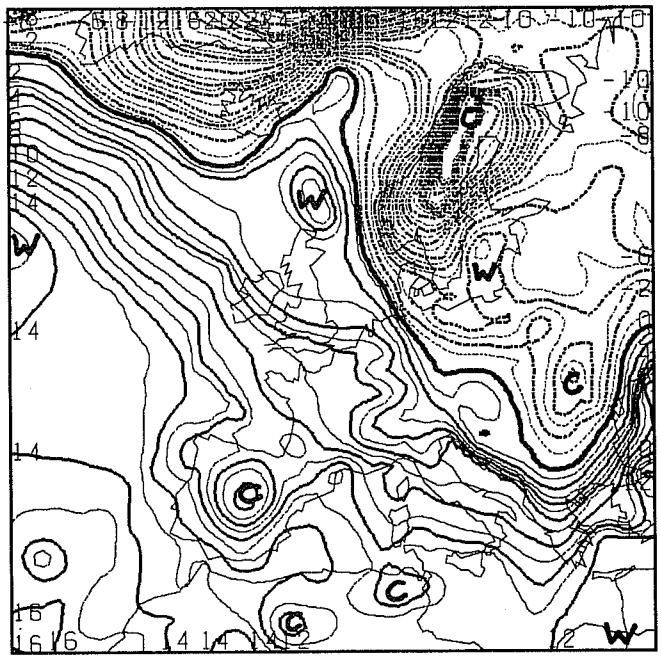

FIG. 9 . TEMPERATURE DGR C.
ANALYSIS 12 GMT 19. 1.1981
PRESSURE-LEVEL 1000. MB

Geopotential height and temperature at 1000 mb as analysed by the fine mesh scheme on isentropic surfaces.

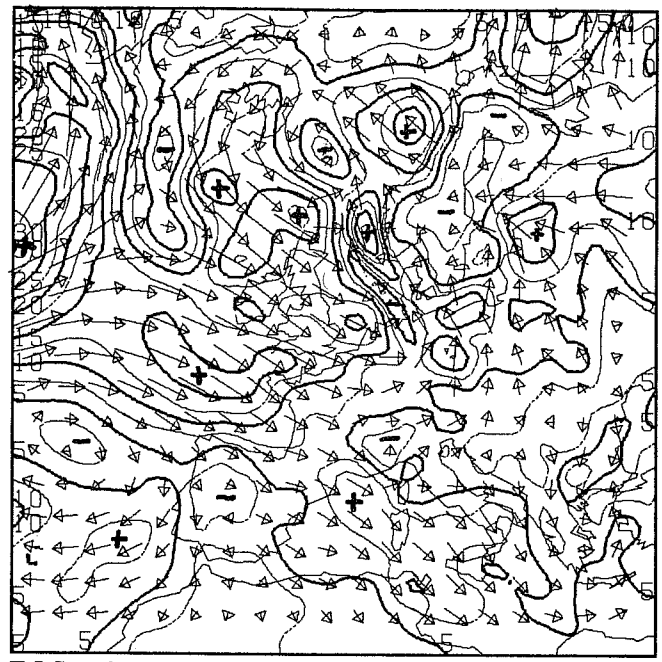

FIG. 10 . ISOTACHS M/SEC
ANALYSIS 12 GMT 19. 1.1981
PRESSURE-LEVEL 1000. MB

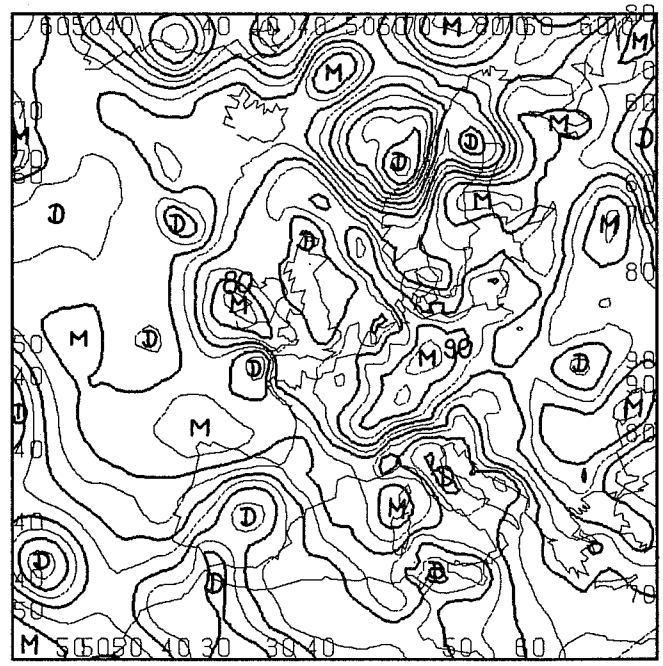

FIG. 11 . REL.HUMIDITY 0/0
ANALYSIS 12 GMT 19. 1.1981
PRESSURE-LEVEL 850. MB

Rotational part of the horizontal wind vector and relative humidity at 1000 mb and 850 mb as analysed by the fine mesh scheme.

For the representation of atmospheric humidity, different types of variables have been used. However, absolute measurements of humidity, like mixing ratio (van Maanen, 1980) or precipitable water, are unfavourable for interpolation on sloping isentropic surfaces, because the strong vertical gradients will overcome the fine mesh interpolation. Therefore relative humidity has been chosen as the variable with the advantage that it is possible to fix its range of values. The vertical check takes into account whether there is saturation.

To get realistic humidity patterns in data sparse areas, schemes have been developed which combine the forecast and observed humidity fields, (Atkins, 1974 or Kästner, 1974); but for the example above, the Cressman scheme gives a first guess of the humidity field on the coarse mesh. Fig. 11 presents the fine mesh result, which is in good agreement with cloud observations and the satellite IR-image (Reimer, 1982).

	First guess	Final analysis
Surface		
unreduced pressure	45%	53%
potential temperature	72%	85%
u - component	49%	62%
v - component	50%	65%
relative humidity	33%	42%
Troposphere		
Montgomery potential	91%	91%
Exner function	75%	91%
stability	24%	70%
u - component	56%	61%
v - component	56%	62%
relative humidity	47%	77%

Fig. 12 Parts of observed variances used in the analysis scheme 19.1.81. 12 GMT

Fig. 12 shows the percentage of observed variances of surface and isentropic variables used for the analysis, where the first guess is represented by the 4-dimensional data assimilation from DWD. With the exception of the Montgomery potential, a larger part of the variance has been utilized for the fine-mesh analysis. However, these mean variances are determined for the observational network and looking at Fig. 6 and 8 reveals that the geopotential analysis has

improved the smaller features by vertical adjustment. The large differences in vertical stability are caused by the fact that 7 pressure levels are used for the coarse-mesh analysis compared with about 14 isentropic levels (which depend very strongly on the analysis of stability) for the fine-mesh representation of the troposphere.

However, it should be stated that deviations between analysis fields and observations can exhibit large absolute values, which should not be regarded as being due only to errors, because radiosonde observations often include very strong vertical gradients or features of a smaller scale (i.e. relative humidity) which would require a finer resolution.

5. FURTHER REMARKS

The partitioning of the analysis procedure into a broad-scale part and a fine mesh correction seems to be useful.

The 4-dimensional analysis used as first guess guarantees an adequate representation of variables in data sparse regions. The remarkable differences between the DWD-analyses and the observations are mainly the result of using isentropic surfaces; the coordinate tends to accommodate special temperature patterns, (like fronts, the tropopause or inversions) which only can be presented by a much higher number of pressure levels.

In general, these deviations are small with the effect that the statistical correction scheme has to be relatively simple, because all observational errors and small scale features are included and the statistical parameters are not precisely known. Therefore several data checks have to be invoked to separate errors.

Another advantage in the use of isentropic surfaces is due to the interpolation on the sloping surfaces, where variables are related in the vertical, so that surface observations are directly combined.

At the moment a more complicated interpolation scheme for the fine mesh corrections might not be useful (with the exception of constructing more detailed autocorrelation curves). The more urgent problem is the physical adjustment of mass and wind field on the fine mesh grid, which is done in a separate step. For that purpose the above scheme is being tested to give fine mesh analyses by the correction of the ageostrophic wind from the operational forecast model of DWD.

REFERENCES

Atkins, . 1974 Objective analysis of relative humidity. Tellus, 26, 6, 663-671.

Bleck, R. 1975 An economical approach to the use of wind data in optimum interpolation of geo- and Montgomery-potential fields. Mon. Wea. Rev., 103, 807-816.

Cressman 1959 An operational objective analysis system. Mon. Wea. Rev., 87, 367-374.

Eddy, A. 1967 The statistical analysis of scalar fields. J. Appl. Meteor., 6, 597-609.

Gandin, I.S. 1963 Objective analysis of meteorological fields. Israel program of scientific translations. Jerusalem 1965.

Hilt, E. and E. Reimer 1982 Improvement of numerical finemesh analysis of humidity using IR-image of NOAA6 satellite data. Analen der Meteor., 18, 61-64.

Kästner, 1974 Ein verfahren zur numerischen analyse der relativen feuchte. Arch. Met. Geoph. Biokl., A, 23.

Lorenc, A. 1980 Design of ECMWF analysis scheme. Data assimilation methods. Seminar 1980, ECMWF, U.K.

Reimer, E. 1980 A test of objective meteorological analysis with optimum utilization of Radiosonde network in Central Europe. Beitr. Phys. Atm., 53, 311-335.

Shapiro, M. 1975 The simulation of upper-level frontogenesis with a 20-level isentropic coordinate primitive equation model. Mon. Wea. Rev., 103, 591-604.

Schlatter, 1975 Some experiment with multivariate statistical objective analysis scheme. Mon. Wea. Rev., 103, 246-257.

Tarbell, et al. 1981 The initialisation of meso-scale weather prediction models using satellite data and precipitation data. Proceedings of Internat. Symposium, 1981, Hamburg.

van Maanen, J. 1980 Objective analysis of relative humidity. GARP WGNE Report No. 20, 38-40.